Monatsh Chem (2011) 142:399–410
DOI 10.1007/s00706-011-0482-x

ORIGINAL PAPER

Interactions of pyridinecarboxylic acid chelators with brain metal ions: Cu(II), Zn(II), and Al(III)

Éva Sija · Annalisa Dean · Tamás Jakusch · Valerio B. Di Marco · Alfonso Venzo · Tamás Kiss

Received: 23 September 2010 / Accepted: 24 February 2011 / Published online: 24 March 2011

Abstract The interactions of Cu(II), Zn(II), and Al(III) with 1,6-dimethyl-4-hydroxy-3-pyridinecarboxylic acid (DQ716) and 2,6-dimethyl-3-hydroxy-4-pyridinecarboxylic acid (DT726), possible chelating agents in Alzheimer's disease, were investigated in aqueous solution. The proton dissociation constants of the ligands, the stability constants, and the coordination modes of the metal complexes formed were determined by pH-potentiometric, UV–vis spectrophotometric, and ^{1}H NMR methods. The nitrogen of the pyridine ring changes the proton affinity of the carboxylate and phenolate moieties and these pyridine derivatives form stronger complexes with Cu(II), Zn(II), and Al(III) than salicylic acid. Interactions of the ligands with human serum albumin as their potential transporter in blood were investigated at physiological pH through ultrafiltration by UV–vis and fluorescence spectroscopy.

É. Sija · T. Jakusch · T. Kiss (✉)
Department of Inorganic and Analytical Chemistry,
University of Szeged, P.O. Box 440, Szeged 6701, Hungary
e-mail: tkiss@chem.u-szeged.hu

A. Dean · V. B. Di Marco (✉)
Department of Chemical Sciences, University of Padova,
via Marzolo 1, 35131 Padua, Italy
e-mail: valerio.dimarco@unipd.it

A. Venzo
Institute of Science and Molecular Technologies, CNR,
via Marzolo 1, 35131 Padua, Italy

T. Kiss
HAS-USZ Bioinorganic Research Group,
P.O. Box 440, Szeged 6701, Hungary

Keywords Potentiometry · Carboxylate ligands · Ultrafiltration · Fluorescence spectroscopy · Chelation therapy · Human serum albumin

Introduction

A number of age-related degenerative diseases, such as Alzheimer's disease (AD), are becoming progressively more important, especially in Europe and the USA, as a result of the significant increase of life expectancy observed nowadays. Enough experimental evidence has been gathered so far which closely correlates AD with abnormal protein folding (misfolding), driving peptides towards their β-sheet conformation. In turn, in this kind of conformation the peptides have the ability to aggregate giving rise to many different types of supramolecular structures, such as amyloid deposits. The main protein component found in amyloid deposits is a 4-kDa amyloid-β-protein (Aβ) [1, 2] that is generated from a much larger $\sim$100- to 130-kDa amyloid precursor protein (APP) by the proteolytic activity of β- and γ-secretases [3].

Aβ displays high affinity towards Cu(II) and Zn(II) at pH 7.4 [4]. These metal ions can promote the formation of Aβ deposits and oligomers in the brain. Elevated levels of Cu(II), Zn(II), and Al(III) have been already proven in deposits and oligomers [5, 6].

Two main forms of Aβ can be distinguished by electrophoresis: a shorter form, composed of 40 amino acids (Aβ_{40}), and a longer one, composed of 42 amino acids (Aβ_{42}) [7]. Aβ_{42} is more prone to aggregation and more toxic to neurons than Aβ_{40} [8]. In the presence of Cu(II) and H_2O_2, the in vitro Aβ_{42} monomers form cross-linked oligomers that are resistant to proteolysis [9]. The oligomeric forms of Aβ_{42} are proven to be potentially very toxic

[10], as they cause further generation of reactive oxygen species and favour membrane depolarization, protein, DNA, and RNA oxidations, and lipid peroxidation.

Metal-induced precipitation of Aβ can be reversed by chelation [11, 12]. However, chelating agents can disrupt the oxidative activity and break the interaction of these metals with Aβ [13]. These and other observations render chelation therapy a very challenging task for future pharmacological treatments of AD [14, 15]. An ideal chelating agent for AD should be sufficiently small to cross the blood–brain barrier, and it should be non-toxic. Moreover, it should exert specific and moderate, rather than indiscriminate and massive, chelation of excess metals [15]. Ligands with intermediate affinity and appreciable metal selectivity are capable of disrupting a few relevant metal–protein interactions rather than inducing generalized, and thus highly toxic, metal depletion like in the classic chelation therapy. For this reason, such ligands can be referred to as metal–protein attenuating compounds (MPACs) or metal-targeting compounds. One of the targets of an MPAC should be the inhibition of Aβ oligomerization and Aβ-related generation of free radicals that can prevent reactive metals from participating in potentially harmful redox reactions [16].

Several attempts were made to obtain efficient MPACs. The antibiotic clioquinol (5-chloro-7-iodo-8-hydroxyquinoline, CQ) has moderate affinity towards Cu(II) and Zn(II), and it was proven to inhibit metal-induced Aβ aggregation and generation of reactive oxygen species in vitro [17]. Clinical studies were stopped because of the difficulties in preventing diiodo-8-hydroxyquinoline contamination in large-scale chemical synthesis of CQ, but the positive effects of CQ encouraged scientists to design new possible MPACs for therapeutic purposes in AD (e.g. see Ref. [18]). Various other compounds have been prepared and tested in vitro and partly in vivo in different laboratories around the world to remove metal ions from the amyloid oligomers and thus to prevent formation of plaques or to achieve at least a partial resolubilisation of the already formed amyloids [19–21].

Besides the toxicity and metal binding strength, other properties should also be investigated for the ligands to be used as an MPAC or as classic chelating agent. Information about the fate of these new potential drugs in the biological systems is needed. As they are expected to be transported in the blood stream, their interactions with plasma proteins might be important. The most probable transporter molecule in serum is albumin, therefore the interaction with this protein should be investigated. The binding strengths and the sites can be determined by studying competition with different site markers such as warfarin or dansyl-glycine [22, 23].

In this work we focus on a previously poorly investigated class of ligands, hydroxypyridinecarboxylic acids (HPs), which have been proposed by us for the "classic" chelation therapy of iron and aluminium [24]. HPs have several positive properties: a low molecular weight, a negligible or even no toxicity, high affinity towards Fe(III) and Al(III), and absence of redox-cycling under in vivo conditions. Here we investigate if HPs can also be proposed as new potential MPACs that could regulate the metal ion distribution in the neurodegenerative disordered brain. In the present study, we consider 1,6-dimethyl-4-hydroxy-3-pyridinecarboxylic acid (DQ716) and 2,6-dimethyl-3-hydroxy-4-pyridinecarboxylic acid (DT726) (Fig. 1). DQ716 is the most promising HP synthesized so far for the classic chelation therapy, and it was proposed for a pharmacologic experimentation [24]. DT726 is under investigation for this aim, and preliminary data indicate very similar positive properties as for DQ716 [25]. The complexation properties of DQ716 and DT726 with Cu(II) and Zn(II) in aqueous solution were determined by means of pH-potentiometric titrations. Also the Al(III)-DT726 complexes were studied, employing potentiometry, UV–vis, and NMR, with the aim to evaluate DT726 as a classic chelating agent. The interactions of DQ716 and DT726 with human serum albumin (HSA) were studied by ultrafiltration and by UV–vis and fluorescence spectroscopy.

Results and discussion

Potentiometric results

Potentiometric titration of each ligand allowed the determination of some pK_A values, which are reported in the upper part of Tables 1 and 2. The pK_{A1} of DQ716 was too low for a pH-potentiometric determination, and it was therefore obtained by UV–vis. The high acidity for the most protonated forms (H_2L for DQ716, H_3L for DT726) is in agreement with values previously observed for other HPs examined so far [24]. As was justified in previous work [24, 26], the first and the last pK_A of both ligands can be assigned to the carboxylic COOH and to the phenolic OH, respectively, and the intermediate pK_A of DT726

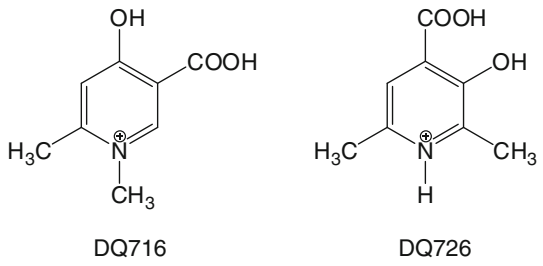

Fig. 1 1,6-Dimethyl-4-hydroxy-3-pyridinecarboxylic acid (DQ716) and 2,6-dimethyl-3-hydroxy-4-pyridinecarboxylic acid (DT726)

Table 1 pK_A values of DQ716 and DT726, and stability constants of Cu(II) and Zn(II) complexes at 25 °C in aqueous KCl 0.2 mol/dm^3

Species	pK_A or log β (uncertainty[a])		
	Salicylic acid[b]	DQ716[c]	DT726[d]
H_3L	–	–	1.21 (5)
H_2L	2.78	<1	6.23 (3)
HL	13.15	6.38 (2)	11.58 (6)
CuLH	–	–	16.08 (2)
CuL	10.62	6.63 (2)	7.58 (13)
$CuLH_{-1}$	–	0.84 (5)	–
CuL_2H_2	–	–	29.89 (24)
CuL_2H	–	–	22.18 (15)
CuL_2	18.45	12.03 (2)	13.26 (12)
$Cu^{2+} + H_3L = Cu(HL) + 2H^+$	–	–	−2.94
$Cu^{2+} + H_2L = CuL + 2H^+$	−5.31	−0.04	–
$Cu(HL) + H_3L = Cu(HL)_2 + 2H^+$	–	–	−5.20
$CuL + H_2L = CuL_2 + 2H^+$	−8.1	−1.27	−7.11
K_d^e (mol/dm^3)	**1.34×10^{-5}**	**5.48×10^{-9}**	**3.42×10^{-5}**
ZnL	6.85	3.91 (5)	6.56 (23)
ZnL_2	–	6.92 (2)	12.12 (28)
ZnL_3	–	8.84 (15)	16.37 (29)
$Zn^{2+} + H_2L = ZnL + 2H^+$	−9.08	−2.76	−6.23
$ZnL + H_2L = ZnL_2 + 2H^+$	–	−3.65	−7.23
$ZnL_2 + H_2L = ZnL_3 + 2H^+$	–	−4.75	−8.54
K_d^e (mol/dm^3)	**7.94×10^{-2}**	**1.32×10^{-4}**	**4.45×10^{-3}**

Values for salicylic acid are reported for comparison. Data are taken from Refs. [42, 43]

[a] Three times the standard deviation

[b] L is the negatively double charged species (L^{2-})

[c] L is the negatively singly charged species (L^-)

[d] L is the negatively doubly charged species (L^{2-})

[e] $K_d = [M]_{free} \sum[H_x L]/\sum[M_w H_y L_z]$ computed at pH 7.4 for $C_M^0 = 25$ μmol/dm^3, $C_L^0 = 50$ μmol/dm^3

(pK_{A2}) to the pyridinic NH. It is worth noting that there is an approximately five orders of magnitude difference in the acidity of the phenolic OH of pyridine (DT726) and of *N*-methylpyridine (DQ716 derivatives), as a result of the positive charge of the methylated nitrogen. The medium has a small but not negligible effect on the acidity of both ligands: pK_A values decrease by ca. 0.2 log units upon increasing the ionic strength from 0.2 mol/dm^3 KCl to 0.6 mol/kg NaCl.

The stoichiometry and the values of the stability constants of the metal–ligand complexes identified in solution are reported in Tables 1 and 2. The representative distribution diagrams are shown in Fig. 2.

As seen from the structural formulae of DQ716 and DT726, both ligands contain a carboxylic and a phenolic function in a reciprocal *ortho* position, i.e. they can be considered as salicylic acid derivatives. Accordingly, their metal ion binding properties were compared to those of salicylate. Differences in the acidity of the functional groups and the resultant proton displacement constants are compared in rows 10, 11, and 16–18 in Table 1 and 17–20 in Table 2. It is seen from the data that both ligands form salicylate-type (COO^-, O^-) mono, bis, and tris complexes depending on the maximum coordination number of the metal ions, and the pyridine-N may be protonated or deprotonated depending on the pH. If the pH ranges of metal complex formation and deprotonation of the pyridine-NH^+ overlap, then protonated complexes are formed, which deprotonate with increasing pH (see Al(III)-ligand systems and Cu(II)-DT726). A comparison of the proton displacement constants reveals that the presence of the pyridinic N in the benzene ring increases the metal binding ability of the salicylate chelating function. This effect appears to be significantly more pronounced when the pyridinic N is methylated.

Although the basic binding mode of the ligands is the same, the speciation showed by the three metal ions and by the two ligands is rather different. As regards Cu(II) + DQ716, only

Table 2 pK_A values of DQ716 and DT726, and stability constants of Al(III) complexes at 25 °C in aqueous NaCl 0.6 mol/kg

Species	pK_A or log β (uncertainty)		
	Salicylic acid[a]	DQ716[b]	DT726
H_3L	–	–	0.66 (18)[c]
H_2L	2.79	0.37 (15)	6.25 (5)
HL	13.4	6.30 (5)	11.44 (3)
AlLH	–	–	18.64 (3)
AlL	13.22	7.66 (3)	–
AlL_2H_2	–	–	35.82 (6)
AlL_2H	–	–	29.44 (18)
AlL_2	23.73	14.38 (1)	–
AlL_2H_{-1}	16.60	–	–
AlL_3H_3	–	–	51.10 (6)
AlL_3H_2	–	–	44.85 (7)
AlL_3H	–	–	37.42 (9)
AlL_3	–	19.37 (1)	29.46 (16)
$AL_2L_2H_{-2}$	17.9	–	–
$Al^{3+} + H_3L = Al(HL)^+ + 2H^+$	–	–	0.68
$Al^{3+} + H_2L = AlL^+ + 2H^+$	−2.71	1.00	–
$Al(HL)^+ + H_3L = Al(HL)_2 + 2H^+$	–	–	−2.14
$AlL^+ + HL = AlL_2 + 2H^+$	−5.42	0.06	–

Values for salicylic acid are reported for comparison

[a] pK_A of free salicylic acid and log β values of Al(III)-salicylic acid [44] refer to a KCl 0.2 mol/dm^3 medium

[b] pK_A values of DQ716 in NaCl 0.6 mol/kg, and stability constants for Al(III)/DQ716, were obtained in a previous work [24]

[c] Value obtained by UV–vis

three complexes were observed. CuL_2 is the main species at slightly acidic and neutral pH values, whereas $CuLH_{-1}$ predominates at higher pH. As the bound ligand has no free protons, $CuLH_{-1}$ can be only the CuL(OH) mixed hydroxo species, in which one of the coordinated water molecules liberates a proton. The pK_A of CuL (5.79) is larger than the pK_A of free Cu(II) in water (ca. 7.2) probably because of an electronic effect exerted by the ligand on the metal centre. A similar speciation is observed for Cu(II) + DT726, but here the complexed ligand is able to deprotonate as it binds the metal ion in its monoprotonated (HL) form resulting in Cu(LH) and $Cu(LH)_2$ species. It is most likely that the pyridinic NH^+ of the ligand remains free. Then $Cu(LH)_2$ deprotonates in a stepwise way with pK values 7.71 and 8.92, significantly higher than that of the non-coordinated pyridinic NH^+ (pK = 6.23), indicating that assignment of the deprotonation constant of the ligand can not be made unambiguously.

Zn(II) forms weak complexes, as they start to have a significant concentration only at pH larger than 3.5–4 (for DQ716) or even at pH larger than 6 (for DT726). Only the simple ZnL, ZnL_2, and ZnL_3 complexes were detected in solution, ZnL_3 being a minor species as it forms at the start of hydroxide precipitation.

Al(III) forms strong complexes with both ligands. For Al(III) + DQ716, a complete discussion can be found in Ref. [24]. DT726 forms a large number of Al(III) complexes, especially in the neutral pH range. The fully coordinated complex AlL_3H_3 is able to deprotonate stepwise at the pyridine rings, producing AlL_3H_2, AlL_3H, and AlL_3. pK_A values are 6.25, 7.43, and 7.96, respectively. The first pK_A is similar to that of free DT726, and the other two increase following the negative charge produced by deprotonation, and in agreement with statistical considerations. The deprotonation of AlL_2H_2 to give AlL_2H (pK_A = 6.38) might occur at the pyridinic nitrogen and/or at a coordinated water molecule (see above).

UV–vis of Al(III)-DT726

UV spectra for Al(III)-DT726 solutions at several pH values are depicted in Fig. 3. Metal complexation affects the typical pyridine ring absorption at around 340 nm, producing a red shift. The following values were obtained for log β (AlLH) and log β (AlL_2H_2): 18.39 (0.03) and 35.67 (0.03). These data are close (0.1–0.3 log units) to the corresponding values obtained by potentiometric titrations (see Table 2). The differences can be attributed to the

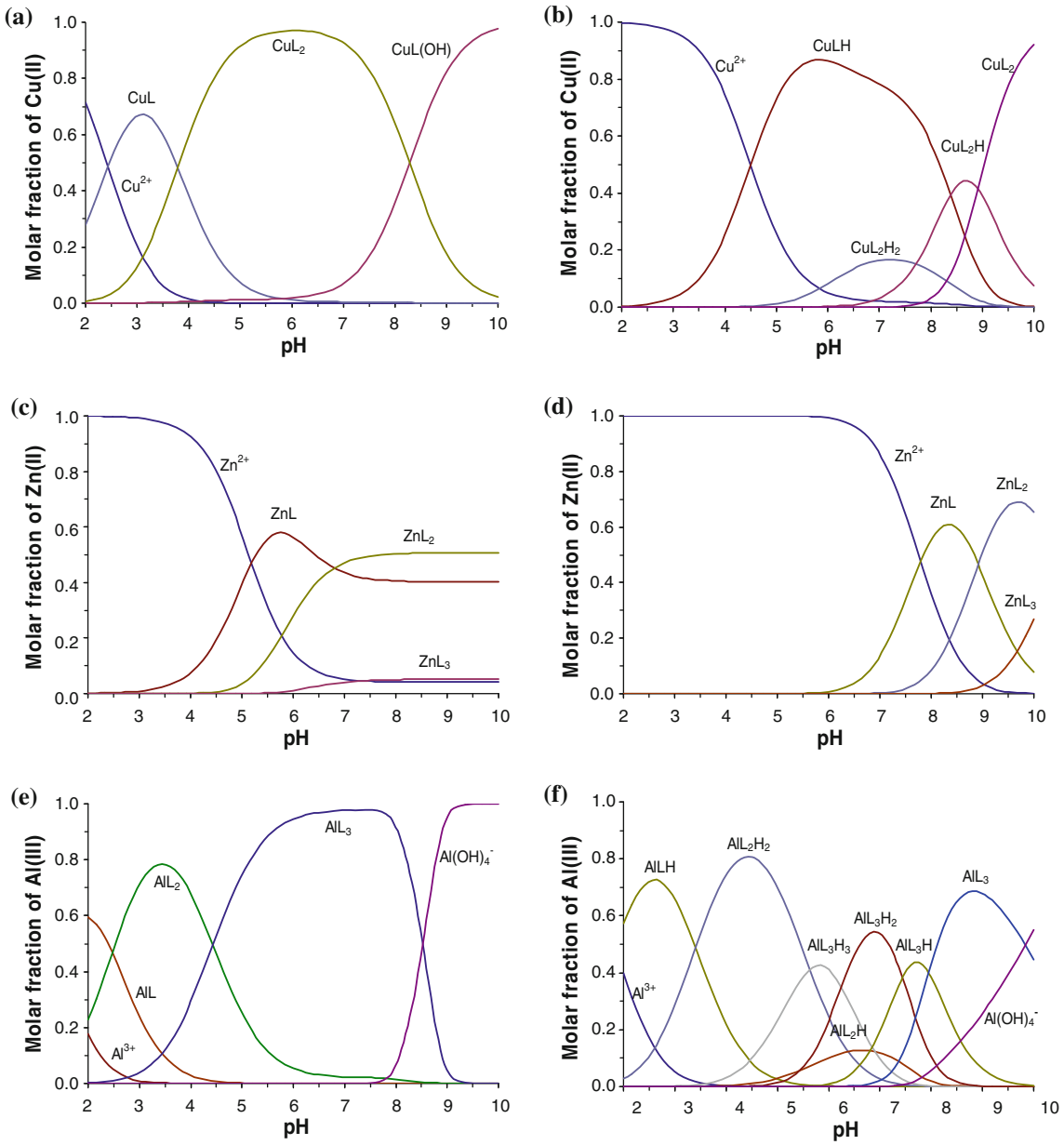

Fig. 2 Distribution diagrams of the most important Cu(II) (**a**, **b**), Zn(II) (**c**, **d**), and Al(III) (**e**, **f**) species in the presence of DQ716 (**a**, **c**, **e**) and DT726 (**b**, **d**, **f**); $C_M^0 = 5 \times 10^{-4}$, $C_L^0 = 2 \times 10^{-3}$ mol/dm^3 or mol/kg

intrinsic uncertainty of these measurements, as the spectral shifts induced by Al(III) complexation are small.

NMR of Al(III)-DT726

The ^{1}H NMR spectra of the free ligand at pD 2.0 show the presence of two singlets, one in the aliphatic zone (6H, $CH_3(2) + CH_3(6)$, δ 2.60) and one in the aromatic zone (1H, H(3), δ 7.81). For pyridine ring numbering see the top of Fig. 4. In principle the two methyl groups are not chemically equivalent because DT726 is not symmetric, but they appear at the same chemical shift. Only at very basic pD values can the two signals be distinguished (spectra not shown), likely because of the deprotonation of the phenolic OH which inductively affects $CH_3(2)$ more than $CH_3(6)$. Upon increasing the pD from 2.0 to 9.4, all signals shift upfield. In agreement with the pK_A values of DT726, the maximum shift is observed at neutral pD: for example, H(5) proton resonates at δ 7.81, 7.80, 7.70, 7.47, and 7.37 ppm at pD 2.0, 3.8, 5.6, 6.8, and 9.4, respectively.

In the presence of Al(III), the resonances of the free ligand are still observed, together with new peaks due to the complexes at all investigated pD values. Figure 4 displays spectra of Al(III)-DT726 solutions.

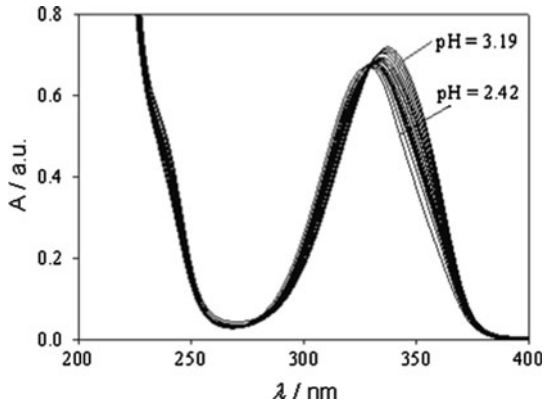

Fig. 3 UV–vis spectra for Al(III)-DT726 solutions at pH = 2.42, 2.48, 2.55, 2.58, 2.62, 2.65, 2.70, 2.74, 2.79, 2.82, 2.85, 2.88, 2.91, 2.95, 2.98, 3.03, 3.07, 3.12, and 3.19. Path cell = 1 cm. Other details are reported in the "Experimental" section

At pD = 2.0 three new narrow signals appear, one in the aromatic region and two in the aliphatic zone. These new peaks can be assigned to AlLH, which according to potentiometric data predominates at this pD. The $CH_3(2)$ and $CH_3(6)$ peaks of the complexed ligand are more resolved than the corresponding signals of the free ligand, probably because of an inductive effect exerted by the metal ion, which is closer to $CH_3(2)$.

At pD values larger than 2.0, further new signals can be observed, most of which are broad. At pD 3.8 the co-presence of AlLH, AlL_2H_2, and AlL_3H_3 is expected on the basis of the potentiometric data. Therefore, the signals should be assigned to these species. A very interesting feature can be observed in the spectrum at pD 5.6, where the complex AlL_3H_3 should predominate. Here, a band composed of at least six to seven singlets appear centred at δ 2.20. Our hypothesis is that this band is composed of eight signals, which have the same intensity, and which can altogether be assigned to the $CH_3(2)$ and the $CH_3(6)$ of AlL_3H_3. DT726 is asymmetric, thus it may chelate the metal, forming AlL_3H_3 in two different spatial configurations. If the three ligands chelate the metal ion in the same configurations, a symmetrical diastereoisomer (AlL_3H_3-sym) forms, and the protons are chemically equivalent. If one ligand chelates differently from the other two, an unsymmetrical diastereoisomer (AlL_3H_3-unsym) forms, and the protons should give rise to different signals in the NMR spectrum. As two different protons are there ($CH_3(2)$ and $CH_3(6)$), eight signals are expected. The signals have about the same intensity: this can be explained by supposing that the formation microconstants of AlL_3H_3-sym and AlL_3H_3-unsym are very similar, so that their ratio in solution is the statistical 1:3 one. Similar ^{1}H NMR patterns have been observed previously for the AlL_3-type complexes of other HPs [24 and references therein]. These signals separate into two groups (having the same intensity) when the pH is increased to pD 6.8 and (even more) to pD 9.4, probably because the deprotonation of the pyridine ring (leading to AlL_3H_2, AlL_3H, and AlL_3) differentiates $CH_3(2)$ from $CH_3(6)$. In the aromatic zone, a multiplet composed of at least three peaks forms, this shape being due to four H(3) signals of AlL_3H_3 according to the previous hypothesis.

NMR data were treated also in a semiquantitative way, by integrating the signals of the free ligand and those of the complexed ligand. Because of partial overlap among these signals, the calculation was performed only at pD 2.0 and 3.8. At pD 2.0, the signals of AlLH account altogether for 20% of the total NMR signal: this value agrees well with the corresponding number, 24.7%, which can be computed from potentiometric data, and which represents the ratio between complexed and total ligand. At pD 3.8, the two numbers (NMR integration ratio and potentiometric ratio) are 43 and 49.4%, respectively. The semiquantitative agreement among two different techniques suggests the absence of systematic errors in our results.

HSA–ligand interaction through ultrafiltration

In order to determine the maximum number of DT726 molecules binding to HSA and the strength of the interaction, evaluation using centrifugal devices with ultrafiltration coupled with UV spectrophotometric was performed. The stoichiometry and the conditional stability constants calculated from the distribution data are listed in Table 3.

Albumin is able to bind up to four DT726 molecules with high affinity at pH 7.40. In order to check the correctness of the calculation, the "formation function" obtained by using the measured equilibrium concentrations of the free and bound ligands together with those calculated from the conditional binding constants determined is presented in Fig. 5.

On the other hand, DQ716 does not exhibit a measurable tendency to bind to HSA, and for this reason constants for HAS-DQ716 species could not be determined. One possible explanation of the different behaviour of the two ligands might lie in the different charges carried by the pyridine ring of the two ligands at pH 7.40: for DT726 the pyridine ring is neutral, for DQ716 it is positively charged. Thus, its affinity to the hydrophobic binding site of HSA decreases.

There are two major drug binding regions on the albumin molecule. One is the warfarin site (warfarin and azopropazone binding area), also called site I. The other is the diazepam site (indole and benzodiazepine binding area), also called site II [27, 28]. Site I was shown to prefer large heterocyclic and negatively charged compounds,

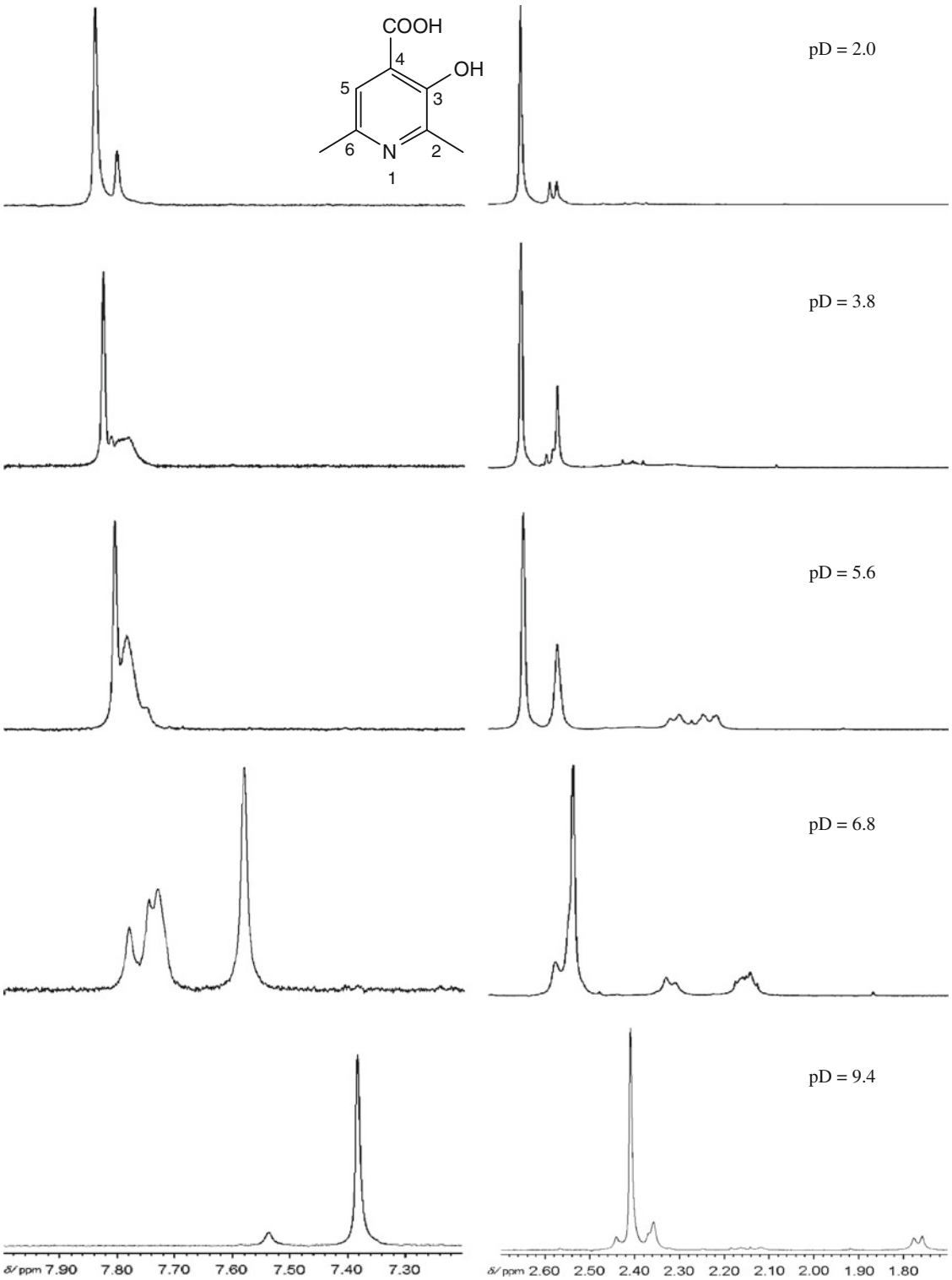

Fig. 4 ^{1}H NMR spectra of D_2O solutions containing Al(III) ($C^0_{Al} = 2.0 \times 10^{-3}$ mol/kg) and DT726 ($C^0_L = 8.0 \times 10^{-3}$ mol/kg) at pD = 2.0, 3.8, 5.6, 6.8, and 9.4. Only the aromatic and the aliphatic zone of the spectra are shown

whereas site II is the preferred site for small aromatic carboxylic acids. Hydrophobic interactions seem to be important at both sites, and thus further details about the actual binding sites of our molecules can be obtained only by competition measurements of the different site markers. Such studies are in progress in our laboratories.

Table 3 Conditional overall and stepwise stability constants (log β', log K') of HSA–ligand (L = DT726) complexes calculated from ultrafiltration-UV measurements

	Log β'_n	Log K'
(HSA)-L	4.83 (9)	4.83
(HSA)-L_2	9.1 (3)	4.27
(HSA)-L_3	13.1 (1)	4.0
(HSA)-L_4	16.1 (6)	3

Measurements were performed at pH 7.40 (HEPES 0.10 M) and $T = 25$ °C. Uncertainties in the stability constants (as ±3 SD values) are given in parentheses

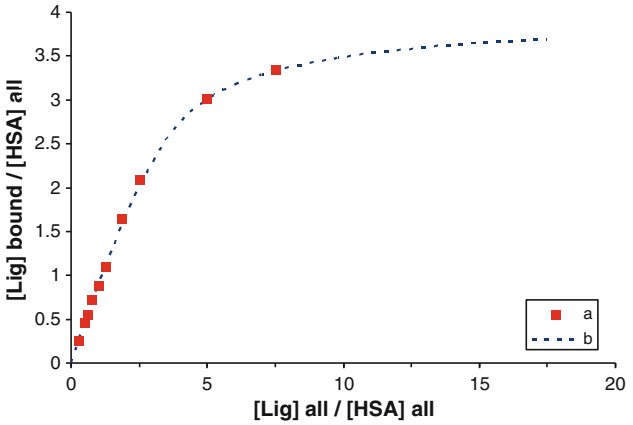

Fig. 5 Equilibrium concentration of the bound ligand/total HSA versus free ligand/total HSA (ligand = DT726): **a** (*squares*) measured by UV spectrophotometry; **b** (*dashed line*) calculated with the conditional binding constants given in Table 3

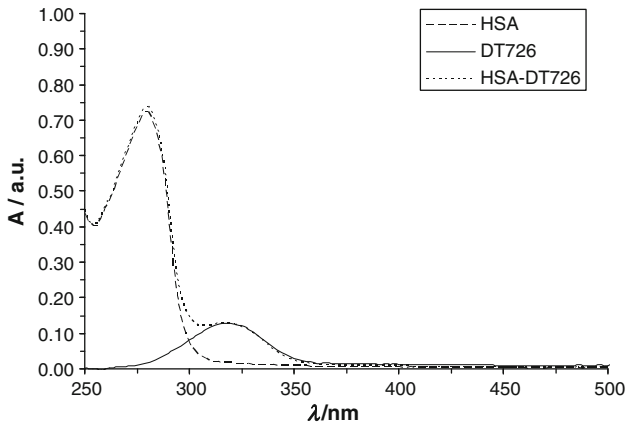

Fig. 6 Absorption spectra of DT726, HSA, and DT726 in the presence of HSA. $C^0_{HSA} = 2 \times 10^{-5}$ mol/dm^3, $C^0_{DT726} = 2 \times 10^{-5}$ mol/dm^3 in 0.1 mM HEPES buffer 7.4 and 25 °C

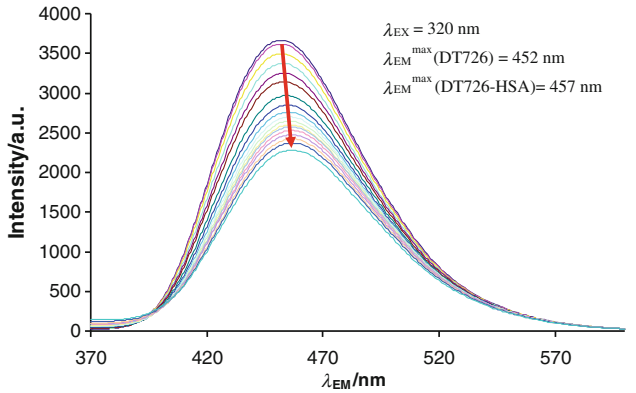

Fig. 7 Fluorescence emission spectra of DT726 as a function of HSA concentration in 20 mM HEPES buffer pH 7.4 and 25 °C. The HSA concentration was increased from 0 to 16 μM and at the same time the concentration of the ligand decreased from 1.5 to 1.2 μM in the direction of the *arrow*

HSA–ligand interaction through fluorescence

Fluorescence spectroscopy has been the most widely used spectroscopic technique for monitoring drug binding to plasma albumin because of its sensitivity, accuracy, rapidity, and ease of use [29].

The absorption of DT726 is characterized by a strong band at 320 nm but it has no absorption in the range of 390–600 nm. The HSA and HSA-DT726 adduct have no absorption at 320 nm and in the examined emission range (see Fig. 6).

A set of emission spectra of DT726 at various concentrations of HSA are shown in Fig. 7. The maximum of emission wavelength shifts from 452 to 457 nm in the presence of HSA. This shift indicates a small structural change (microenvironment) of HSA upon interaction with DT726 that can be rationalized in terms of interactions between DT726 and HSA in the ground state and formation of a complex.

Other information that is shown by the spectra, when HSA is added to the solution containing DT726, is that the fluorescence intensity of DT726 decreased continuously with increasing concentration of HSA. The fluorescence quenching spectra of DT726 with varying concentrations of HSA are shown in Fig. 7. The observed behaviour suggests that complexes are formed between DT726 and HSA, which are responsible for the fluorescence quenching of DT726.

The calculated molar emission spectrum of the ligand alone agrees very well with the experimental one. At the same time the emission intensity maximum of DT726 in the presence of HSA is shifted to 457 nm indicating the interaction between the two components (Fig. 8).

The calculated log β is 5.80 ± 0.01. The values reported in the literature [30–32] for the interaction of HSA with various antibiotic drugs are of the order of 10^3–10^5. It has to be noted that this value is one order of magnitude higher than that obtained by ultrafiltration (see above), and that the interaction of only one DT726 could be detected by

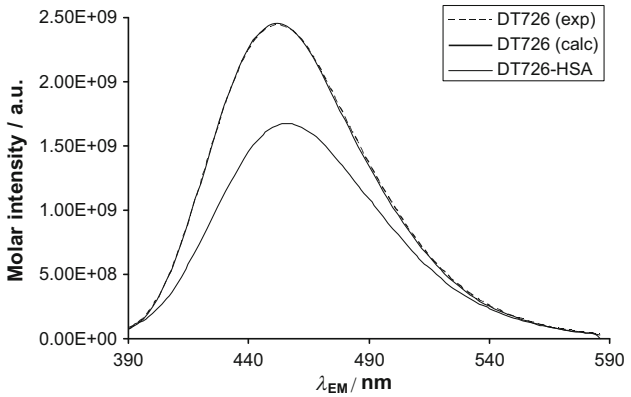

Fig. 8 Calculated and experimental molar emission spectra of DT726 (which coincide) and DT726-HSA adduct

fluorescence, instead of four ligands as found by ultrafiltration. This difference can be explained by the three orders of magnitude difference in the concentration range of the measurement: ultrafiltration characterises the system in the millimolar range, whereas fluorescence works at the micromolar range and was not able to detect the formation of polynuclear species.

Discussion of the chelation strength towards metal ions

The metal binding strength of the various chelator molecules towards the metal ions can be compared in different ways. Biologists prefer to use K_D, the dissociation constant, which gives the extent of dissociation at given experimental conditions (C_M^0, C_L^0, pH) and can be calculated from the thermodynamic stability constants (see footnote of Table 1). The K_D values have been calculated for the Cu(II) and Zn(II) complexes, as we have reasonably good indicator values for their potential applicability as metal ion modulators in AD [11].

Another parameter used to characterised the complexation strength of different ligands towards a given metal ion (preferably used by chemists) is the pM graph ($pM = -\log [M_{free}]$) as a function of pH. The larger the pM, the stronger is the binding strength of the ligand. pM graphs of our ligands for the metal ions studied are displayed in Fig. 9.

The pM graphs demonstrate that both HPs form stronger complexes than salicylic acid does with all considered metal ions and over all the pH range. The stability increase with respect to salicylic acid can be attributed to the nitrogen of the pyridine ring: its positive charge reduces the proton affinity of the carboxylate and phenolate moieties, without affecting (or affecting to a minor degree) their metal ion affinity, in the same way as happens when passing from catechol to hydroxypyridinones [33]. In previous complexation work regarding Fe(III) and Al(III) [24, 34] we observed that the methylation of the pyridine ring of HPs increases the metal ion affinity even more, because of the electron donor properties of the methyl group(s), and we found that the stability increase is maximum if the methyl group is at position 1 (i.e. bound to nitrogen). The pM graphs in Fig. 9 show that DQ716 forms stronger complexes with Cu(II), Zn(II), and Al(III) than DT726 does: this result further supports our previous finding.

Application as metal–protein attenuating compounds

The dissociation constants for 1:1 Cu(II)-Aβ and Zn(II)-Aβ complexes reported in the literature [11], computed at pH 7.4 as K_D values, vary with the type of buffer used in the measurements and the methods employed for their determination. Faller and Hureau [11] suggest that a good MPAC should have K_D values of around 1–10 pmol/dm^3 and 0.1–10 μmol/dm^3 for Cu(II) and Zn(II), respectively. Table 1 shows that both DQ716 and DT726 have larger values than these, i.e. these ligands chelate Cu(II) and Zn(II) too weakly and cannot efficiently remove the metal ions from Aβ. For this reason, it is likely that DQ716 and DT726 cannot be proposed as MPACs for the therapy of AD.

Nevertheless, the weakness of the Cu(II) and Zn(II) complexes formed by DQ716 and DT726, together with the strength of their Al(III) (and Fe(III)) complexes), confirms that they can be selective drugs for the classic chelation therapy of iron and aluminium. In principle they are able to remove iron and aluminium from the body without significantly affecting copper and zinc metabolism.

Experimental

Compounds

The pH-metric titrations were performed with 0.2 mol/dm^3 KOH solution or 0.1 mol/kg NaOH prepared from KOH (Merck) and NaOH pellets (Fluka). The base was standardised against HCl solutions prepared from 36% HCl (Merck). The 0.1 mol/dm^3 metal ion solutions were prepared from $AlCl_3 \cdot 6H_2O$ (Fluka), $CuCl_2$, and $ZnCl_2$ (Aldrich), and their exact concentrations were determined gravimetrically via the oxinates. DQ716 [24] and DT726 [25] were obtained by synthesis, and their solutions were standardised against base.

Solutions for UV–vis were the same as for potentiometric titrations. Solutions for ^{1}H NMR measurements were prepared by dissolving weighed amounts of DT726 and $AlCl_3$ (Carlo Erba) in D_2O (Aldrich, 99.9% atom D). The internal reference was $Me_3SiCH_2CH_2COOH$ (TSP, Aldrich).

Solutions for fluorescence measurements were prepared using the ligands, HEPES (Sigma), and HSA (Sigma). HSA solutions were freshly prepared just before the measurements.

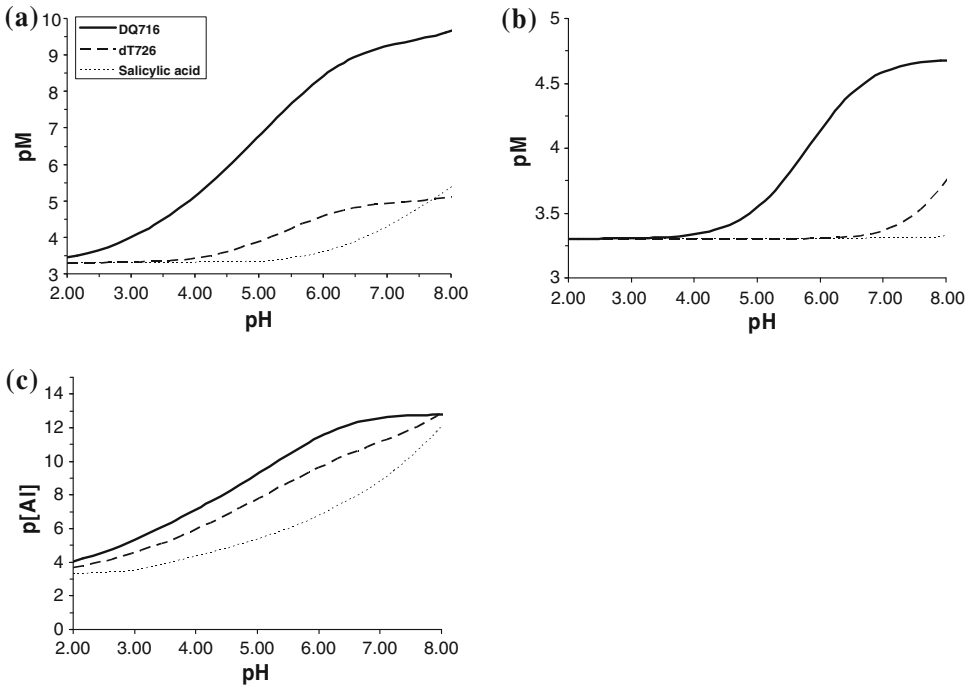

Fig. 9 pM versus pH at $C_M^0 = 2 \times 10^{-3}$, $C_L^0 = 5 \times 10^{-4}$ mol/dm^3 or mol/kg, M = Cu(II) (**a**), Zn(II) (**b**), Al(III) (**c**)

Equilibrium measurements

The stability constants of the proton and metal complexes of the ligands were determined by pH-potentiometric titrations of 20-cm^3 samples. A Radiometer pHM 84 instrument equipped with a Metrohm combined electrode (type 6.0234.110) and Metrohm 715 Dosimat burette was used for the pH-metric measurements. The samples were in all cases thermostatted at 25.0 ± 0.1 °C, and completely deoxygenated by bubbling purified argon for ca. 15 min before the measurements. Argon was also passed over the solutions during the titrations. The electrode system was calibrated according to Irving et al. [35] and the pH-metric readings could therefore be converted into hydrogen ion concentration. About 200 titration points were used for each system. The accepted fitting of the titration curves was always less than 0.01 cm^3. Duplicate titrations were performed. The reproducibility of the titrations was within 0.005 pH units. The pH-metric titrations were performed in the pH range 2.0–11.0 or until precipitation occurred in the samples. The ligand concentrations varied in the range 1.00×10^{-3}–4.00×10^{-3} mol/dm^3. The metal ion to ligand ratios was in the range 1:1–1:4. After the mixing of Al(III) and DT726 in an acidic solution (pH ca. 3), the measured pH drifted and reached a constant value only after ca. 1 h, suggesting a low complex formation rate. The kinetics of the Al(III) + DT726 reaction became "normal" (equilibration after ca. 1 min) at pH values above 3. These findings are in agreement with previous results with other HPs [24 and references therein]. Experimental details regarding the handling of the slow kinetics during the titrations are reported elsewhere [36].

For Cu(II)- and Zn(II)-related titrations, the ionic strength of the solutions was adjusted to 0.2 mol/dm^3 KCl, and a 0.2 mol/dm^3 carbonate-free KOH solution was the titrant. For Al(III)-related titrations, medium was a 0.6 mol/kg NaCl aqueous solution, and the titrant was a 0.1 mol/kg carbonate-free NaOH solution. A 0.6 mol/kg NaCl ionic strength (=0.594 mol/dm^3) was used to allow a rigorous comparison among Al(III) data which have always been obtained in this medium ([24] and references therein). The water ionization constant, pK_w, is 13.76 ± 0.01 in KCl 0.2 mol/dm^3, and 13.69 ± 0.01 in NaCl 0.6 mol/kg.

The general equilibrium reaction is: $pM + qL + rH = M_pL_qH_r$, where M denotes the metal ion and L the non-protonated ligand molecule (see footnote of Table 1). Charges are omitted for simplicity. The corresponding concentration stability constants $\beta_{pqr} = [M_pL_qH_r]/[M]^p[L]^q[H]^r$ were calculated using the PSEQUAD computer program [28]. Calculations were always made on the experimental results obtained before precipitation. pK_A values were calculated from the protonation constants obtained by PSEQUAD and refer to the general reaction: $H_hL = H_{h-1}L + H$.

UV–vis spectra were recorded at 25 °C using a Perkin-Elmer Lambda 20 spectrophotometer operating in a NaCl 0.6 mol/kg medium. For free DT726, solutions were prepared dissolving 1.39×10^{-4} mol/kg of DT726 and varying the pH between 0.3 and 1.1. Here the pH was computed from the stoichiometric concentration of HCl,

because the [H^+] modifications produced by the other species were negligible under these conditions. For Al(III) + DT726, two solutions were prepared. In the first, 1.08×10^{-3} mol/kg of Al(III) and 1.06×10^{-3} mol/kg of DT726 were dissolved, the pH was between 2.4 and 3.2. In the second, 5.53×10^{-4} mol/kg of Al(III) and 1.08×10^{-3} mol/kg of DT726 were dissolved, the pH was between 2.9 and 4.5. Calculations of the stability constants were performed at the wavelength displaying the maximum absorbance variation with pH (338 and 350 nm for free DT726; 310, 328, 341, and 350 nm for Al(III) + DT726).

^{1}H NMR spectra were obtained at 25 °C using a Bruker DRX-400 spectrometer operating at 400.13 MHz. Chemical shift values are given in δ units with reference to internal TSP. Suitable integral values for the proton signals were obtained by a prescan delay of 10 s. The assignment of the proton resonances was performed by standard chemical shift correlations and NOESY measurements when necessary. Spectra were collected in D_2O solutions containing free DT726, or Al(III) + DT726. The pH was measured with a Crison 5014 combined glass electrode previously calibrated in buffered aqueous solutions at pH = 4 and pH = 7. The values of pD were computed by adding 0.41 pH units to the pH meter readings, to correct for isotopic and solvent effects due to the use of D_2O instead of H_2O [37].

Fluorescence measurements

Fluorescence spectra were measured with an Hitachi F4500 fluorescence spectrophotometer using quartz cuvettes of 1-cm optical path and operating at 25 °C. For the measurements of the free ligand (DT726), 2.0 cm^3 of a 1.5 or a 3 μmol/dm^3 ligand solution were placed into the cell. Titrations of DT726 solutions in 20 mM HEPES buffer (pH 7.4) were performed adding 80 μM HSA stock solution directly to the cuvette. The concentration of DT726 changed between 1.5–1.2 and 3.0–2.4 μmol/dm^3. The fluorescence emission spectra were registered after 5 min. An excitation wavelength of 320 nm was selected and the fluorescence spectra were recorded in the range of 390–600 nm. The fluorescence intensities were corrected for DT726 absorption of exciting light [38]:

$$F_{\text{corr}} = F_{\text{obs}} \times 10^{-\varepsilon c l} \quad (1)$$

where F_{cor} and F_{obs} are the fluorescence intensities corrected and observed, respectively; ε is the molar absorption coefficient at 320 nm; $l = 1.0$ cm (the optical path); and c the DT726 concentration. The molar absorption coefficient was determined by UV–vis spectrometry, that is calculated as 4,792 M^{-1} cm^{-1}. The intensity of fluorescence used in this paper is the corrected fluorescence intensity [39].

The calculations were performed with the aid of the PSEQUAD computer program [40, 41]. We supposed that the two emitting forms are the DT726 and DT726-HSA adduct.

Ultrafiltration

Samples were separated by ultrafiltration through 10-kDa membrane filters (Microcon YM-10 centrifugal filter unit, Amicon, Millipore) according to a standard procedure [41]. In the protein–ligand interaction studies, all 0.50-cm^3 samples contained 200 μM HSA and the carrier ligand in 0.10 M HEPES buffer at pH 7.4. The ligand concentrations were varied from 50 μM to 1 mM. Time-dependent measurements were carried out to determine the time needed to reach equilibrium between the reacting partners. An incubation time of 20 min was found to be enough for attaining true equilibrium. The samples were then transferred to filter tubes and centrifuged for 10 min at 10,000 rpm (25 °C). After the separation, the low molecular mass (LMM) fractions were obtained. The non-bound ligand was determined by UV spectrophotometry. Control samples containing the carrier ligand and HEPES at the same concentrations but without the protein were used to determine the accurate analytical concentration of the ligand. No adsorption of the drug on the filter was observed. The binding constants were calculated with the computer program PSEQUAD [40] from the total and free concentration data pairs obtained at different protein–ligand ratios.

Acknowledgments The work was made in the frame of the CNR-HAS Bilateral Research Program, and was also supported by the Hungarian Research Funds (TÁMOP 4.2.1/B. and OTKA K77833). This paper was also supported by the János Bolyai Research Scholarship of the Hungarian Academy of Sciences (TJ). The project named "TÁMOP-4.2.1/B-09/1/KONV-2010-0005 – Creating the Center of Excellence at the University of Szeged" is supported by the European Union and co-financed by the European Regional Fund.

References

1. Glenner GG, Wong CW (1984) Biochem Biophys Res Commun 120:885
2. Masters CL, Simms G, Weinman NA, Multhaup G, McDonald BL, Beyreuther K (1985) Proc Natl Acad Sci U S A 82:4245
3. Checler F (1995) J Neurochem 65:1431
4. Atwood CS, Scarpa RC, Huang X, Moir RD, Jones WD, Fairlie DP, Tanzi RE, Bush AI (2000) J Neurochem 75:1219
5. Lovell MA, Robertson JD, Teesdale WJ, Campbell JL, Markesbery WR (1998) J Neurol Sci 158:47
6. Bush IA (2003) Trends Neurosci 26:207
7. Klafki HW, Wiltfang J, Staufenbiel M (1996) Anal Biochem 237:24
8. Hureau C, Faller P (2009) Biochimie 91:1212
9. Atwood CS, Perry G, Zeng H, Kato Y, Jones WD, Ling KQ, Huang X, Moir RD, Wang D, Sayre LM (2004) Biochemistry 43:560

10. Fang CL, Wu WH, Liu Q, Sun X, Ma Y, Zhao YF, Li YM (2010) Regul Pept 163:1
11. Faller P, Hureau C (2009) Dalton Trans 2009:1080–1094
12. Atwood CS, Moir RD, Huang X, Bacarra NME, Scarpa RC, Romano DM (1998) J Biol Chem 273:12817
13. Cuajungco MP, Faget KY, Huang X, Tanzi RE, Bush AI (2000) Ann N Y Acad Sci 920:292
14. Crichton RR, Ward RJ (2006) Metal-based neurodegeneration: from molecular mechanisms to therapeutic strategies. Wiley, Chichester
15. Bolognin S, Drago D, Messori L, Zatta P (2009) Med Res Rev 29:547
16. Bush IA, Tanzi RE (2008) Neurotherapeutics 5:421
17. Cherny RA, Atwood CS, Xilinas ME, Gray DN, Jones WD, McLean CA, Barnham KJ, Volitakis I, Fraser FW, Kim YS (2001) Neuron 30:665
18. Adlard PA, Cherny RA, Finkelstein DI, Gautier E, Robb E, Cortes M, Volitakis I, Liu X, Smith JP, Perez K, Laughton K, Li QX, Charman SA, Nicolazzo JA, Wilkins S, Deleva K, Lynch T, Kok G, Ritchie CW, Tanzi RE, Cappai R, Masters CL, Barnham KJ, Bush AI (2008) Neuron 59:43
19. Hindo SS, Mancino AM, Braymer JJ, Liu Y, Vivekanandan S, Ramamoorthy A, Lim MH (2009) J Am Chem Soc 131:16663
20. Lakatos A, Zsigó É, Hollender D, Nagy NV, Fülöp L, Simon D, Bozsó Zs, Kiss T (2010) Dalton Trans 39:1302
21. Green DE, Bowen ML, Scott LE, Storr T, Merkel M, Bohmerle K, Thompson KH, Patrick BO, Schugar HJ, Orvig C (2010) Dalton Trans 39:1604
22. Sudlow G, Birkett DJ, Wade DN (1975) Clin Exper Pharmacol Physiol 2:129
23. Muller N, Lapicque F, Drelon E, Netter P (1994) J Pharm Pharmacol 46:300
24. Dean A, Ferlin MG, Brun P, Castagliuolo I, Yokel RA, Badocco D, Pastore P, Venzo A, Bombi GG, Di Marco VB (2009) Dalton Trans 2009:1815–1824
25. Dean A, Di Marco VB (in preparation)
26. Di Marco VB, Yokel RA, Ferlin MG, Tapparo A, Bombi GG (2002) Eur J Inorg Chem 2002:2648–2655
27. Sudlow G, Birkett DJ, Wade DN (1975) Mol Pharmacol 11:824
28. Sudlow G, Birkett DJ, Wade DN (1976) Mol Pharmacol 12:1052
29. Seedher N, Bhatia S (2006) Pharmacol Res 54:77
30. Bi S, Song D, Tian Y, Zhou X, Liu Z, Zhang H (2005) Spectrochim Acta A 61:629
31. Chengnong Y, Jinqiang T, Dan X, Yi L, Zuting P (2006) Chin J Anal Chem 34:796
32. Ahmad B, Parveen S, Khan RH (2006) Biomacromolecules 7:1350
33. Scarrow RC, Riley PE, Abu-Dari K, White DL, Raymond KN (1985) Inorg Chem 24:954
34. Di Marco VB, Dean A, Ferlin MG, Yokel RA, Li H, Venzo A, Bombi GG (2006) Eur J Inorg Chem 2006:1284–1293
35. Irving HM, Miles MG, Pettit LD (1967) Anal Chim Acta 38:475
36. Di Marco VB, Tapparo A, Bertani R, Bombi GG (1999) Ann Chim (Rome) 89:535
37. Covington AK, Paabo M, Robinson RA, Bates RG (1968) Anal Chem 40:700
38. Whalley CV, Rankin SM, Hoult JRS, Jessup W, Leake DS (1990) Biochem Pharmacol 39:1743
39. Epps DE, Raub TJ, Caiolfa V, Chiari A, Zamai M (1999) J Pharm Pharmacol 51:41
40. Zékány L, Nagypál I, Peintler G (1991) Technical software distribution, Baltimore
41. Enyedi ÉA, Farkas E, Dömötör O, Santos MA (2011) J Inorg Biochem 105:326
42 Kurz H (1986) In: Reidenberg MM, Erill S (eds) Drug protein binding. Praeger, New York, p 70
43 Martell AE, Smith RM (1982) Critical stability constants, vol 5. Plenum, New York
44 Kiss T, Atkári K, Jezowska-Bojczuk M, Decock P (1993) J Coord Chem 29:81